

# A Model-based Reconstruction Technique for Inversion Recovery Prepared Radially Acquired Data

Johannes Tran-Gia<sup>1</sup>, Dietbert Hahn<sup>1</sup>, and Herbert Köstler<sup>1</sup>  
<sup>1</sup>Institute of Radiology, University of Würzburg, Würzburg, Germany

**Introduction:** MR parameter mapping is usually performed by tracking the evolution of the magnetization after a suitable preparation. Especially for short relaxation times, this can be difficult and measurements have to be performed in segmented fashion or with low spatial resolution. In [1], we proposed a Model-based Acceleration of Parameter mapping (MAP) algorithm in conjunction with radial data acquisition, capable of fully resolving an exponential signal evolution after saturation magnetization preparation. In this work, the MAP technique was extended for inversion recovery (IR) prepared datasets. This allows quantifying  $T_1$  from a radial single-shot dataset using only one single magnetization preparation.

**Materials and Methods:** According to [2], the magnetization  $M(TI)$  in an IR snapshot FLASH experiment can be modeled by the mono-exponential function

$$M(TI) = M_0^* - (M_0 + M_0^*) \cdot \exp(-TI/T_1^*) \quad (1)$$

( $TI$ : inversion time,  $M_0$ : equilibrium magnetization,  $T_1^*$ : apparent relaxation time,  $M_0^*$ : steady-state magnetization of the tissue in presence of continuous RF excitation). Utilizing this model as prior knowledge allows characterizing  $M(TI)$  by only the three parameters  $M_0$ ,  $M_0^*$  and  $T_1^*$ . For small flip angles  $\alpha$ , these parameters can be used to derive the actual longitudinal relaxation parameter

$$T_1 = T_1^* \cdot [(M_0 + M_0^*)/M_0^* - 1]. \quad (2)$$

In this work, Eq. 1 was included in the MAP algorithm presented in [1] in order to fully resolve the evolution of the signal after IR magnetization preparation from only one single IR preparation.

The proposed IR-MAP technique reconstructs one image for every acquired radial projection as well as an  $M_0$ ,  $M_0^*$  and  $T_1^*$  map. It is initialized by separately gridding every single projection of the radially acquired k-space data using self-calibrating GROG [3] and Fourier transforming these k-spaces into image space. Subsequently, a least-squares fit of Eq. 1 is applied pixel by pixel, yielding a set of parameters  $M_0(x, y)$ ,  $M_0^*(x, y)$  and  $T_1^*(x, y)$  for every pixel  $(x, y)$ , corresponding to one model image for the contrast of every acquired projection. In order to ensure data consistency, every originally measured projection is substituted into the k-space of its model image. The consistent model images are then passed on to the subsequent iteration (Fig. 1). All reconstructions in this study were terminated after a fixed number of 500 iterations.

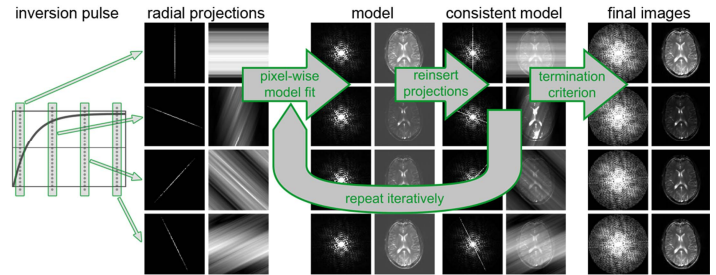


Fig. 1: Basic IR-MAP reconstruction scheme.

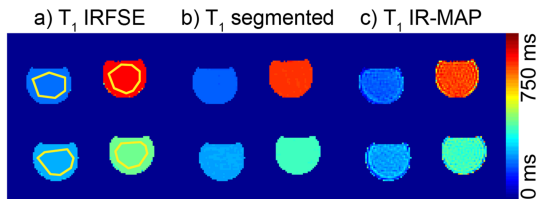


Fig. 2:  $T_1$  maps of the phantom measurements.

position	a) $T_1$ IRFSE	b) $T_1$ segmented	c) $T_1$ IR-MAP
top left	173 ± 0	155 ± 1	156 ± 12
bottom left	216 ± 0	211 ± 1	205 ± 15
bottom right	361 ± 0	320 ± 2	318 ± 19
top right	649 ± 0	613 ± 3	603 ± 19

Table 1: Means & standard deviations of the phantom.

Measurements of a human brain were carried out with the radial IR snapshot FLASH sequence described above (1024 radial projections, total scan time = 6.8 s) and again, the IR-MAP algorithm and Eq. 2 were used for image reconstruction and  $T_1$  quantification. Due to the long scan time, a segmented IR snapshot FLASH measurement was not feasible for the in-vivo measurements. In consequence, the echo train length of the Cartesian IRFSE experiment was increased to 32 for a reduction in scan time to about 25 min for the acquisition of 24 contrasts with  $TI \in [100 \text{ ms}, 8000 \text{ ms}]$  and a reference  $T_1$  map was obtained.

**Results & Discussion:** Figure 2 shows  $T_1$  maps obtained from the reference IRFSE dataset (a), the segmented radial IR snapshot FLASH dataset (b) and the IR-MAP reconstructed single preparation dataset (c). The ROIs used for the evaluation are indicated in yellow. Table 1 lists the mean  $T_1$  values and their standard deviations (STD) within the compartments obtained in the ROI analysis. Results of the in-vivo measurements are depicted in Fig. 3. Shown are the IRFSE reference (a) as well as the IR-MAP reconstructed  $T_1$  map obtained from only one single magnetization preparation (b).

The  $T_1$  values in Table 1 show a good agreement between the segmented (b) and the IR-MAP reconstructed (c)  $T_1$  maps obtained with the IR snapshot FLASH acquisition. The increased STD within the ROIs of (c) are caused by the drastically reduced amount of preparations (1 vs. 202) used for the reconstruction. However, they are still acceptably small especially with respect to the acquisition time of more than 3 h for the segmented compared to 3.4 s for the single-preparation dataset and demonstrate the functionality of the IR-MAP algorithm. The IRFSE  $T_1$  maps of the phantom and in-vivo measurements indicate a systematic underestimation of the  $T_1$  maps obtained in the IR snapshot FLASH experiments. This might be a combination of inaccuracies in the IRFSE method on one side and limits of Eq. 2 in order to derive  $T_1$  out of the apparent relaxation parameters time  $M_0$ ,  $M_0^*$  and  $T_1^*$  on the other side.

In conclusion, the proposed IR-MAP reconstruction algorithm allows quantifying the longitudinal relaxation parameter  $T_1$  from one single magnetization preparation, leading to extremely short acquisition times of about 7 s for a human brain. Compared to the SR preparation used in the first MAP implementation in [1], the signal-to-noise ratio is increased by a factor of approximately 2.

**Acknowledgements:** Johannes Tran-Gia was supported by a grant of the German Excellence Initiative to the Graduate School of Life Sciences, Würzburg.

**References:** [1] Tran-Gia et al., Proc ISMRM 20:359 (2012), [2] Deichmann et al., J Magn Reson 96:608-612 (1992), [3] Seiberlich et al., Magn Reson Med 59:930-935 (2008), [4] Winkelmann et al., IEEE T Med Imaging 16:68-76 (2007)

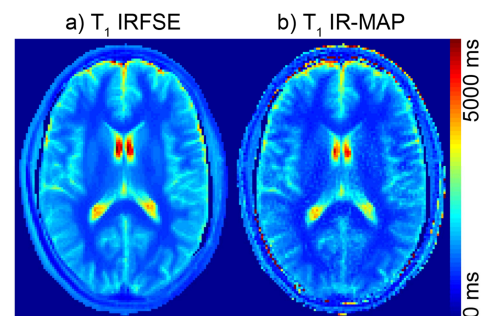


Fig. 3:  $T_1$  maps of the in-vivo measurements.